

RESEARCH PAPER



## Baicalin reversal of DNA hypermethylation-associated Klotho suppression ameliorates renal injury in type 1 diabetic mouse model

Xiao-Tan Zhang<sup>a,b,\*</sup>, Guang Wang<sup>a,\*</sup>, Liu-Fang Ye<sup>a</sup>, Yu Pu<sup>a</sup>, Run-Tong Li<sup>a</sup>, Jianxin Liang<sup>a</sup>, Lijun Wang<sup>c</sup>, Kenneth Ka Ho Lee<sup>d</sup>, and Xuesong Yang<sup>a,e</sup>

<sup>a</sup>International Joint Laboratory for Embryonic Development & Prenatal Medicine, Division of Histology and Embryology, Medical College, Jinan University, Guangzhou, China; <sup>b</sup>Department of Clinical Pathology, The First Affiliated Hospital of Jinan University, Guangzhou, China; <sup>c</sup>Department of Public Health, Medical College, Jinan University, Guangzhou, China; <sup>d</sup>Key Laboratory for Regenerative Medicine of the Ministry of Education, School of Biomedical Sciences, Chinese University of Hong Kong, Shatin, Hong Kong; <sup>e</sup>Key Laboratory for Regenerative Medicine of the Ministry of Education, Jinan University, Guangzhou, China

### ABSTRACT

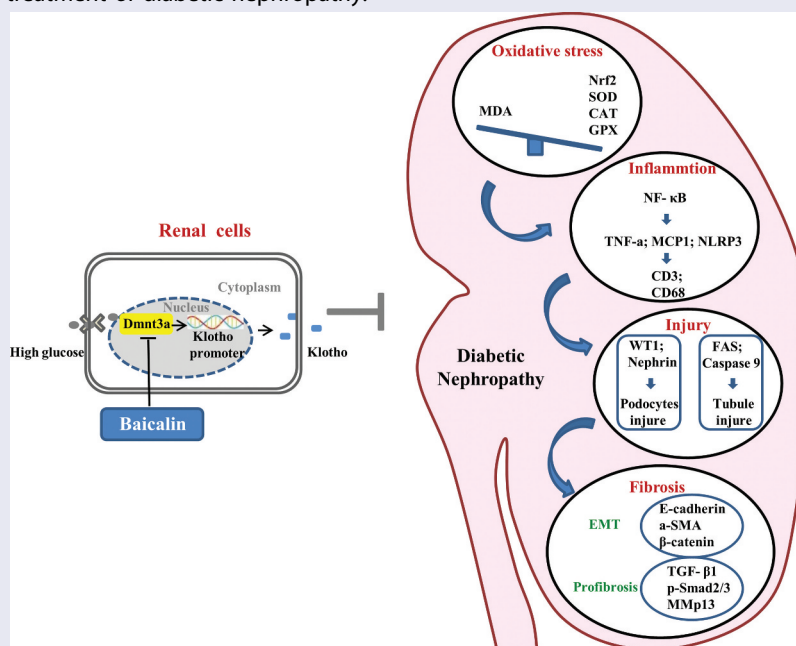
Baicalin is a flavone glycoside that possesses numerous pharmacological properties. but its protective mode of action in kidney injury induced by diabetes mellitus remains incompletely understood. Using a streptozotocin (STZ)-induced diabetic mouse model, we found that baicalin could ameliorate diabetes-induced the pathological changes of the kidney function and morphology through suppressing inflammation and oxidative stress. Furthermore, baicalin treatment could alleviate interstitial fibrosis in the diabetic kidney via inhibiting epithelial-to-mesenchymal transition (EMT), which was accompanied by a sharp upregulation of Klotho, the endogenous inhibitor of renal fibrosis. We further verified that baicalin-rescued expression of Klotho was associated with Klotho promoter hypomethylation due to aberrant methyltransferase 3a expressions. Klotho knockdown via RNA interferences largely abrogated the anti-renal fibrotic effects of Baicalin in HK2 cells. These findings suggested that baicalin could alleviate renal injury-induced by diabetes through partly modulating Klotho promoter methylation, which provides new insights into the treatment of diabetic nephropathy.

### ARTICLE HISTORY

Received 16 January 2020  
Revised 22 September 2020  
Accepted 27 October 2020


### KEYWORDS

Diabetes; kidney; fibrosis;  
DNA methylation; Klotho



**CONTACT** Xuesong Yang  [yang\\_xuesong@126.com](mailto:yang_xuesong@126.com)

\*These authors contributed equally to this work

 Supplemental data for this article can be accessed [here](#).

© 2020 Informa UK Limited, trading as Taylor & Francis Group

## Introduction

The prevalence and incidence of diabetes mellitus (DM) has increased significantly worldwide, diabetes mellitus (DM) and hypertension are considered as the most common causes of end-stage renal disease (ESRD)[1]. Hadjadj S et al found ESRD occurred in 75 patients with type 2 diabetes and 112 with type 1 diabetes, translating to an incidence rate of 18.4 vs 47.1 per 1,000 patient-years in type 2 diabetes vs type 1 diabetes, respectively [2]. Diabetic nephropathy (DN) is characterized by proteinuria, glomerular hypertrophy, glomerular basement membrane thickening, podocyte injury, extracellular matrix extension, glomerular sclerosis, and tubulointerstitial fibrosis [3]. The pathogenesis of diabetic nephropathy remains obscure because of the complexity, including genetic, hemodynamic factors, cytokines, metabolic disorders, abnormal signaling pathway activation, inflammation, oxidative stress, DNA damage and so on. All of those factors might participate in the development of the disease and ultimately lead to kidney damage [4–6]. Many signaling pathways have been reported to be involved in diabetic kidney disease development including ROS, activation of protein kinase C (PKC) and transforming growth factor  $\beta$  (TGF $\beta$ ), mitogen-activated protein kinase (MAPK) signaling pathways, and activation of nuclear factor- $\kappa$ B (NF- $\kappa$ B), which is a pro-inflammatory transcription factor that activates expression of inflammatory-associated genes [7]. The Klotho is tightly correlated with the pathogenic mechanism of chronic kidney disease [8], because it could inhibit TGF- $\beta$ 1 receptors by directly binding to these receptors to block the TGF- $\beta$ 1 signaling pathway [9]. Furthermore, epigenetic regulation, which involves the switching on and off of gene expressions dictated by signaling pathways and micro-environmental stimuli has also been implicated diabetic kidney disease [10]. For instance, global DNA hypermethylation has been determined to be proportionally higher in patients mortality with chronic kidney disease [11].

Many people with type 1 diabetes (T1DM) are associated with diabetic complications including

kidney disease. However, the underlying mechanisms and corresponding treatments are still controversial. Growing studies revealed that it was related to the enhanced inflammation and oxidative stress level, implying that the drug monomers with anti-inflammatory and antioxidant effects might have therapeutic potential in the treatment of T1DM [12–14]. Baicalin is a flavone glycoside and has called a glucuronide of baicalein. It is created through the binding of glucuronic acid with baicalein, a flavone present in the roots of *Scutellaria baicalensis* and *Scutellaria lateriflora*. Baicalin is mainly employed as a herbal supplement for maintaining health and treating diseases such as anti-neuroinflammation [15], antioxidant, cancer [16] anxiety [17], improving lung function [18] and infertility [19] in Asian countries. To date, the most acceptable mechanism for baicalin's bioactivities is its effects as an anti-oxidant and anti-inflammatory agent [20]. Excessive reactive oxygen species (ROS) production and chronic inflammation are considered to be key factors inducing renal injury. Hence, we investigated whether or not baicalin could prevent renal injury in type 1 diabetes mellitus mice model in this study.

## Materials and methods

### Experimental animal

The Chinese Kunming mouse, a outbred mouse strain, was started from Swiss mice brought to Kunming, China, from the Indian Haffkine Institute in 1944 [21–23]. Kunming mice have many advantages such as good quality, high disease resistance, strong adaptability, and rapid growth rates. Nowadays, Kunming mice have been widely used as an animal model in the study of various diseases, such as the disorders in central nervous system, anxiety, diabetes, etc [24–26]. The Kunming mice used in this study were obtained from the Laboratory Animal Center at Sun Yat-sen University (Guangzhou, China). These mice were housed in the animal facility under constant room temperature, humidity (50–60%), 12:12 hour light-dark cycle, and supplied with standard food pellets and water.

### **Model of type 1 diabetes**

Eight-week-old female mice were used to induce diabetes mellitus by injecting STZ (Sigma-Aldrich, St. Louis, MO, USA; dissolved in 0.01 mol/l citrate buffer, pH 4.5) at 75 mg/kg body weight for three consecutive days. Blood glucose levels were measured using the Roche Accu-Chek Aviva Blood Glucose System (Roche, Penzberg, BY, Germany) for 7 days after STZ injection. The mice with blood glucose level exceeding 16 mM were considered as type-1 diabetic, and used in subsequent experiment [27]. Normal mice (n = 11) were assigned to the control group that exclusively received vehicle.

### **Drug administration and experimental design**

Baicalin (99% purity) was purchased from Santa Cruz Biotechnology (sc-204,638, Dallas, TX, USA; dissolved in 0.1% DMSO). Diabetic mice were randomly assigned to the following: Diabetes mellitus group (DM group, n = 9); DM + Baicalin group (n = 7): the mice were gavaged at 1 mL/(kg•d) for 7 days, once a day (the total amount of baicalin required for one mouse per day is 40 mg/kg) [28]. In control (n = 11) and DM groups, the mice were administered with 0.1% DMSO via an intra-gastric gavage for 1 week.

### **Pathophysiological examinations**

The body weights (BW) of the mice were recorded 24 h prior to euthanasia. The mice were housed individually in metabolic cages and water consumption over 24 h and the quantity of urine produced were recorded. After euthanization, the kidneys were removed, decapsulated, and weighed. The left kidney was harvested for histology and immunohistological staining, while the right kidney was processed for RNA or protein analysis.

### **Renal function analysis**

Blood samples were centrifuged for 10 min at 3000 rpm and blood serum creatinine, blood urea nitrogen (BUN), urinary creatinine, and

albumin levels were determined using an automatic biochemistry analyzer (Roche Diagnostic Systems, cobas8000 c702, Japan). The analysis was conducted according to instructions supplied by the manufacturer (n = 6/group). Mouse urinary ACR (UACR) was calculated as  $ACR = \text{urinary albumin/urinary creatinine (mg/mg)}$ .

### **Histology**

Briefly, 12-week-old mouse kidneys (control, STZ-induced-diabetes mellitus, and STZ-induced-diabetes mellitus with Baicalin treatment) were fixed in 4% paraformaldehyde at 4 °C for 24 h. The specimens were then dehydrated, cleared in xylene and embedded in paraffin wax. The embedded specimens were serially sectioned at 5 μm using a rotary microtome (Leica, Germany). The sections were stained with hematoxylin and eosin (H&E), periodic acid Schiff (PAS) reaction, Masson's trichrome dyes (Masson staining), Sirius Red, or immunohistochemically. The Masson and Sirius Red stains were used to reveal the presence of fibrosis in kidney sections and also any other histological alterations. Photographs were captured of the stained histological sections using an epifluorescence microscope (Olympus IX51, Leica DM 4000B).

### **Histological assessments of renal glomerulus and tubules**

To determine the extent of collagen deposit and fibrosis in the kidney tissues, we established a mesangial matrix index. This index was statistically established from measurements of kidney sections stained using Periodic acid-Schiff dyes as previously reported [29]. The mean glomerular basement (GBM) thickness was determined by measuring 50 different randomly selected sites on transverse sections of the kidneys, using Image Pro Plus software as previously reported [29]. We also developed an renal tubule damage score by histologically assessing the extent of tubulointerstitial injury

and fibrosis. Briefly, 20 high magnification fields of the corticomedullary region in each kidney section were randomly selected and blindly scored by an independent observer. The total renal tubule injury was divided into classes 0 to 3, based on the percentage of normal tubules and tubular dilatations. The classification of tubular epithelial cell damage was graded as following: 0 = absent; 1 = 1–25%; 2 = 26–50% and 3 > 50% of fibrotic tubule area in the total field observed [30].

### **Immunofluorescent stainings**

Longitudinal sections of mouse kidneys were dewaxed in xylene, rehydrated, and then heated in the microwave for antigen retrieval in citrate buffer (pH = 6.0). The sections were then exposed to 3% hydrogen peroxide for 10 min to block endogenous peroxidase. Nonspecific immunoreactions were blocked using 5% inactivated goat serum in PBS for 30 min at room temperature. The sections were then washed in PBS and incubated with the appropriate primary antibody of interest: WT1 (1:100, Invitrogen, PA5-16,879, USA), LTL (1:100, Vector lab, FL-1321, USA), PCNA (1:200, Abcam, ab29, UK), Caspase-9 (1:100, Cell Signaling Technology, USA), CD3 (1:100, Abcam, ab16669, UK), CD68 (1:50, Bioss, bs-20,402 R, China), P65 (1:100, Cell Signaling Technology, #6956, USA),  $\alpha$ -SMA (1:100, Abcam, ab5694, UK), TGF- $\beta$ 1 (1:1000, Abcam, ab64715, UK), E-Cadherin (1:100, DSHB, USA),  $\beta$ -catenin (1:100, Abcam, ab32572, UK) and Atg7 (1:100, ABGENT, USA) antibodies overnight on a shaker at 4 °C. The sections were washed extensively and incubated in horseradish peroxidase (HRP) goat anti-rabbit IgG secondary antibody (1:400, EarthOx, USA) for 3 h at room temperature inside a dark box, and then visualized with DAB (Maixin, China). The immunostained sections were counterstained with hematoxylin. For intensity analysis, CD3 and CD68 expressions were selected for semiquantitative analysis by H-SCORE [31]. For immunofluorescent staining, the sections after treatment with the primary antibodies

were incubated with corresponding alexa fluor 555 or 488 secondary antibodies (1:1000, Invitrogen, USA) at room temperature for 2 hours on a shaker. All the immunofluorescently stained sections were counterstained with DAPI (1:1000, Invitrogen) at room temperature for 1 h.

### **Transmission electron microscopy(TEM)**

Kidney tissues were fixed in 2.5% glutaraldehyde and embedded in Epon. The specimens were ultra-thin-sectioned, stained, and examined under a transmission electron microscope (FEI, TECNAI12, USA).

### **Western blotting**

Western blotting was performed using standard procedures. The antibodies used specifically recognized Nephtrin (1:500, Bioss, bs-10,233 R, China), WT1 (1:1000, Invitrogen, PA5-16,879, USA), Fas (1:1000, Cell Signaling Technology, USA), Caspase-9 (1:1000, Cell Signaling Technology, USA), PCNA (1:1000, Abcam, ab29, UK), CD3 (1:1000, Abcam, ab16669, UK), CD68 (1:500, Bioss, bs-20,402 R, China), P65 (1:1000, Cell Signaling Technology, #6956, USA), I $\kappa$ B- $\alpha$  (1:1000, Cell Signaling Technology, #4814, USA), Nrf2 (1:1000, Santa Cruz Biotechnology, sc-722, USA), E-cadherin (1:1000, DSHB, USA),  $\alpha$ -SMA (1:1000, Abcam, ab5694, UK),  $\beta$ -catenin (1:1000, Abcam, ab32572, UK), TGF- $\beta$ 1 (1:1000, Abcam, ab64715, UK), p-smad2/3 (1:1000, Cell Signaling Technology, #8828, USA), MMP13 (1:1000, Abcam, ab39012, UK), Dnmt1 (1:500, Bioss, bs-0678 R, China), Dnmt3a (1:500, Bioss, bs-23,029 R, China), Dnmt3b (1:500, Bioss, bs-0301 R, China), Klotho (1:400, Bioss, bs-2925 R, China), Atg7 (1:1000, ABGENT, USA), LC3B (1:1000, Cell Signaling Technology, #2775, USA) and  $\beta$ -actin (1:2000, Proteintech, USA). The proteins were isolated using a radio-immuno-precipitation assay kit (RIPA, Sigma, USA) buffer supplemented with protease and phosphatase inhibitors. The protein concentrations were quantified using a BCA assay kit.

The loading/internal control was  $\beta$ -actin (1:3000, Proteintech, USA). Bio-Rad imaging systems plus Quantity One software (BIO-RAD, USA) was used to capture the chemiluminescent signals and for analyzing the data. All samples were performed in triplicate.

### **RNA isolation and RT-qPCR analysis**

Total RNA was isolated from the kidneys using a Trizol kit (Invitrogen, USA) according to the manufacturer's instructions. First-strand cDNA was synthesized to a final volume of 20  $\mu$ l using an iScript<sup>TM</sup> cDNA Synthesis Kit (BIO-RAD, USA). Following reverse transcription, PCR amplification of the cDNA was performed as described previously [32,33]. SYBR<sup>®</sup> Green qPCR assays were then conducted using a PrimeScript<sup>TM</sup> RT reagent kit (Takara, Japan). All specific primers used are listed in Supplementary Table 1. Reverse transcription and amplification reactions were performed in Bio-Rad S1000<sup>TM</sup> (Bio-Rad, USA) and ABI 7000 thermal cyclers, respectively. The house-keeping gene PPIA was run in parallel to confirm that equal amounts of RNA were introduced in each reaction. The ratio between the intensities of the fluorescently-stained bands corresponding to the genes and PPIA was calculated to quantify the level of gene expression.

### **Malondialdehyde, catalase and superoxide dismutase measurements**

We measured the antioxidase activities including malondialdehyde (MDA), catalase (CAT) and total superoxide dismutase (SOD) in our samples. MDA (A003), CAT (A007) and SOD (A001) assay kits was purchased from Nanjing Jiancheng Bioengineering Institute. Renal tissue samples were prepared from 0.1 g of frozen renal tissues which were homogenized in 1 ml PBS (pH 7.2) and centrifuged at 10,000 g for 15 min at 4 °C. The supernatants were then harvested and kept at -80 °C until used. The MDA, CAT and SOD levels in the renal tissues were analyzed using the

detection kits, according to the manufacturer's instructions.

### **Measurements of DNA methylation levels in gene promoters**

Genomic DNA was isolated from the mouse livers using a TIANamp Genomic DNA Kit (TIANGEN, Beijing, China), and DNA bisulfite conversion was performed as previously described [34]. The chemically modified DNA was subsequently used as a template for direct sequencing to determine the methylation level of the selected CpG sites in the target gene promoters [35]. Briefly, the sequence was retrieved from NCBI at <http://www.ncbi.nlm.nih.gov/gene?>. Primers were designed online via methprimer (<http://www.urogene.org/methprimer/>), and the sequences used are presented in Supplementary Table 2. The product of the target gene promoter was amplified by PCR. For each 25  $\mu$ l PCR reaction, 2.5  $\mu$ l 10X buffer, 2  $\mu$ l dNTPs, 0.125  $\mu$ l Taq Hotstart polymerase (Takara), 1  $\mu$ l 10  $\mu$ M forward primer, 1  $\mu$ l 10  $\mu$ M reverse primer, 2  $\mu$ l DNA template and 16.375  $\mu$ l water were used. The size and quality of the PCR products (5  $\mu$ l) were verified on 2% agarose gels, and the remaining products were purified and directly sequenced.

### **Cell Culture and gene transfection**

Human renal tubular epithelial cells (HK2 cells) were purchased from Guangzhou Jiniou Biotechnology Co., Ltd (Guangzhou, China). The cells were cultured in DMEM (Gibco,

**Table 1.** The renal morphology.

Parameter	Diabetes mellitus		
	Control (n = 6)	(DM) (n = 6)	DM+Baicalin (n = 6)
Glomerular size ( $\mu\text{m}^2$ )	34.51 $\pm$ 6.91	39.26 $\pm$ 4.95**	35.90 $\pm$ 4.72 <sup>#</sup>
Media-to-lumen ratio	0.27 $\pm$ 0.07	0.29 $\pm$ 0.04	0.28 $\pm$ 0.05

Values are given as mean  $\pm$  SEM.

\*p < 0.05, \*\*p < 0.01, \*\*\*p < 0.001 compared with control group;

<sup>#</sup>p < 0.05, <sup>##</sup>p < 0.01, <sup>###</sup>p < 0.001 compared with DM group

Gaithersburg, USA), 10% fetal bovine serum (Gibco, Gaithersburg, USA), 100 U/ml penicillin and 100 µg/ml streptomycin., inside a humidified cell incubator with 5% CO<sub>2</sub> at 37 °C. The cells (1 × 10<sup>6</sup> cells/ml) were maintained in six-well culture-plates and treated with 50 mM glucose or 6 µM Baicalin plus 50 mM glucose. For gene transfection, the HK2 cells were transfected by either Control-siRNA (Invitrogen, Carlsbad, CA, USA) or Klotho-siRNA (5'-GCGACTACCCAGAGAGTAT-3') [36], using lipofectamin 3000 (Invitrogen, Carlsbad, CA, USA).

### Data analysis

The mesangial matrix index was determined by measuring and analyzing the extent of renal interstitial fibrosis, as indicated by Sirius Red positively stained areas, using the Image Pro-Plus 7.0 software [37]. Statistical analyses for all the experimental data generated were performed using a SPSS 13.0 statistical package program for Windows. The data were presented as mean ± SD. All staining was quantified from at least five sections that were at least chosen from per group. Sections were randomly selected and analyzed under blinded conditions. All experiments analyses were repeated at least three times and the representative images were presented eventually. Sample size and P values are presented in Supplementary Table 3–9. Statistical significance were determined using paired T-test, or one-way analysis of variance (ANOVA). P < 0.05 was considered to be significant.

## Results

### Baicalin treatment alleviates renal deficiencies in STZ-induced diabetic mice

To determine whether or not baicalin treatment could alleviate renal deficiencies, we injected baicalin solution (40 mg/kg) daily for seven days into STZ-induced diabetic mice [38–40]. In Figure 1(a) we illustrated how the diabetic mice were produced and the bioactive concentration and timing of baicalin administration, as also previously

reported with some modification [28]. In diabetic mice, consecutive measurements of blood glucose levels revealed that it reached peak level week 10, while baicalin treatment alleviated the peak blood glucose level. Nevertheless, the blood glucose levels in both diabetic treated and untreated groups were significantly higher than control mice when observed 8–12 weeks (Figure 1(b)). We also assay the general status and renal function indexes of control and diabetic mice with/without baicalin treatment. The results revealed that there was significant increase in water consumption, urine volume, ratio of kidney weight/body weight, blood urea nitrogen (BUN), serum creatinine, and urine albumin-to-creatinine (UACR) in diabetic mice as compared with controls and baicalin treated diabetic mice (Figure 1(c-d,g-j)). The body weight decreased even though there was no influence on kidney weight in diabetic mice with baicalin treatment (Figure 1(e-f)). This suggests that baicalin treatment can alleviate deficiencies in renal functions induced by hyperglycemia.

### Pathological and ultrastructural changes in renal glomeruli and tubules in diabetic mice treated with baicalin

We next assessed the morphological changes in renal glomerulus and tubules to evaluate whether or not baicalin administration improved renal insufficiencies in diabetic mice was due to influence on the structures of renal glomeruli and tubules. We found that baicalin treatment repressed diabetes induced glomerulus enlargement (Table 1). Histological examinations revealed that diabetes grossly affected and altered the morphology of the glomerulus, but these diabetes-induced lesions in the glomerulus were repressed following baicalin treatment, as revealed in H&E and PAS stained kidney sections and TEM (Figure 2(a-b)). PAS staining was used to determine the extent of fibrosis because the dyes stains up collagen deposits, so that we were able to construct a renal mesangial matrix index. We determined that the matrix index increased in diabetic mice as compared with normal control mice and

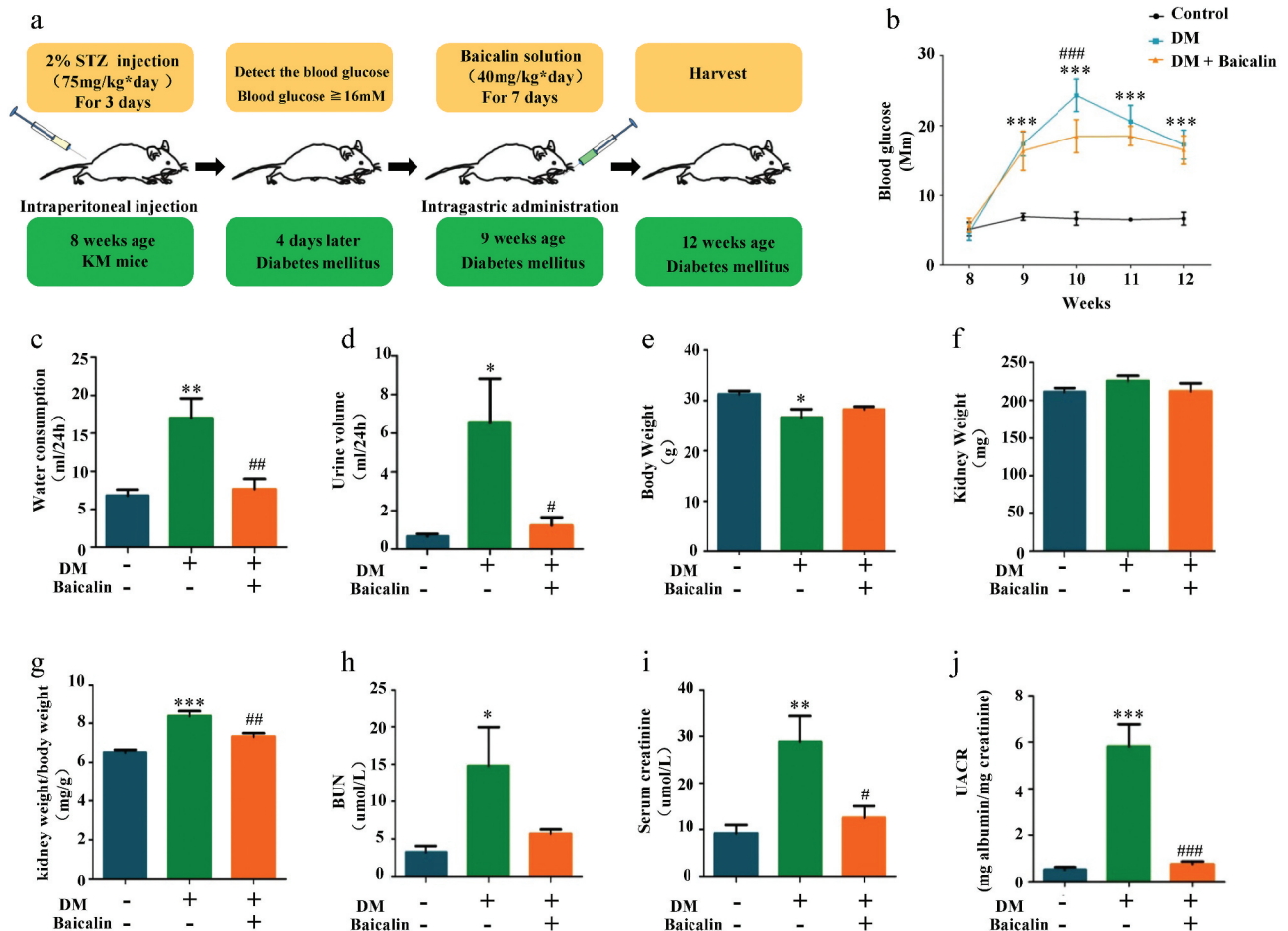


**Figure 1.** Mouse blood glucose levels and renal functions after STZ administration in the absence/presence of baicalin.

**a:** Illustration showing the production of the STZ-induced diabetic mouse model. In addition, timing for blood glucose measurements and baicalin administration. **b:** Graph showing blood glucose levels at week 8–12 following STZ administration amongst controls, DM and DM + Baicalin treatment groups. **c–j:** Bar charts comparing water consumption at 24 hours (c), urine volume at 24 hours (d), body weight (e), kidney weight (f), ratios of kidney and body weights (g), BUN in blood (h), serum creatinine in blood (i), and UACR (j) amongst control, DM and DM + Baicalin groups. Abbreviation: STZ, streptozotocin; BUN, blood urea nitrogen; UACR, urine albumin-to-creatinine ratio. \* $p < 0.05$ , \*\* $p < 0.01$ , \*\*\* $p < 0.001$  compared with control group; # $p < 0.05$ , ## $p < 0.01$ , ### $p < 0.001$  compared with DM group.

baicalin treatment could partially inhibit this increase (Figure 2(a,c)). The TEM kidney sections showed that baicalin reduced the thickness of the glomerular basement membrane induced by hyperglycemia in diabetic mice (Figure 2(b,e)). Podocytes play an important role in maintaining the integrity of glomerular filtration barrier, and accumulating evidence showed that podocyte dysfunction contributed to the pathogenesis of DN [41]. Wilms' tumor 1 (WT1) and Nephrin are important and essential regulators of podocyte function in the glomerulus [42]. Immunofluorescent staining and Western blot analysis revealed that normal

podocytes expressed WT1 but the number of WT1<sup>+</sup> podocytes was significantly reduced in diabetic glomerulus. However, baicalin treatment was able maintain WT1 expression so that there were more WT1<sup>+</sup> podocytes present than in untreated diabetic kidneys (Figure 2(a, d,g-h)). Moreover, RT-qPCR analysis revealed that baicalin treatment inhibited an increase in Col4a1 and Lamb2 expressions induced by hyperglycemia while simultaneously potentiated a reduction in hyperglycemia-induced Nphs1 and Podx1 expression (Figure 2(f)).

H&E staining showed that baicalin could repress renal tubules injury induced by

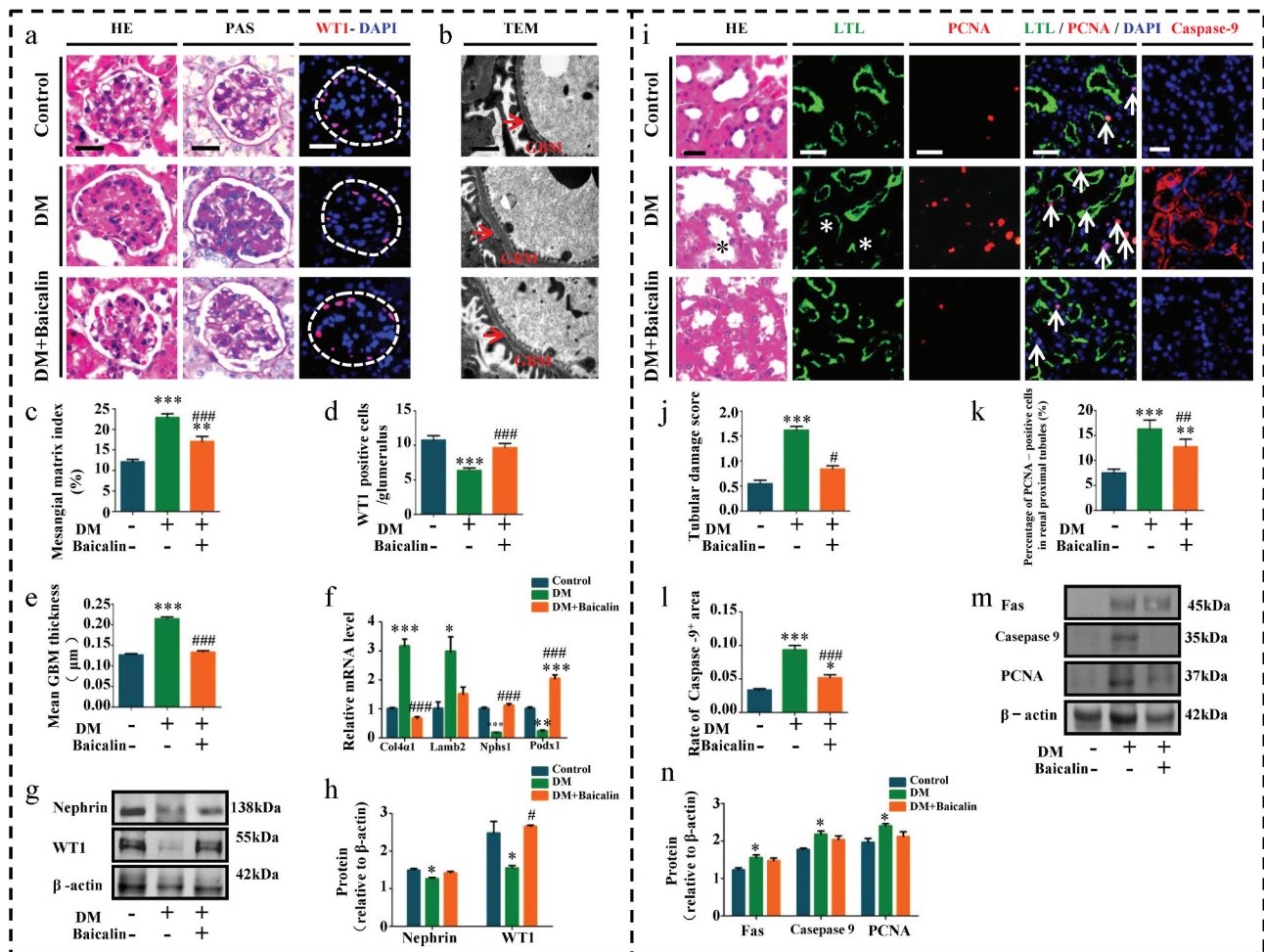


**Figure 2.** Morphology and protein expression changes of renal glomeruli and renal tubules in diabetic mice with baicalin treatment. **a-h:** Morphology and protein expression changes of renal glomeruli in diabetic mice with baicalin treatment. **a:** Representative micrographs of H&E-stained, PAS-stained and WT1 immunofluorescent-stained renal glomeruli from control, DM and DM + Baicalin treated mice. **b:** Representative micrographs of transmission electron microscope renal glomeruli from control, DM and DM + Baicalin treated mice. **c-e:** Bar charts comparing the mesangial matrix index (c), WT1<sup>+</sup> cells (d) and mean GBM thickness (e) among control, DM and DM + Baicalin groups. **f:** RT-qPCR showing extent of Col4a1, Lamb2, Nphs1 and Podx1 expressions. **g-h:** Western blot analysis showing extent of Nephrin and WT1 expressions among control, DM and DM + Baicalin groups. **i-n:** Morphology and protein expression changes of renal tubules in diabetic mice with baicalin treatment. **i:** Representative micrographs of H&E-stained, LTL immunofluorescent-stained, PCNA immunofluorescent-stained, LTL and PCNA double-stained and Caspase-9 immunofluorescent-stained renal tubules from control, DM and DM + Baicalin groups. **j-l:** Bar charts comparing tubular damage scores (j), percentage of PCNA<sup>+</sup>/DAPI tubule cells (k) and percentage of Caspase-9<sup>+</sup>/DAPI tubule cells (l) among control, DM and DM + Baicalin group. **m-n:** Western blot showing the extent of Fas, Caspase-9, and PCNA expressions in control, DM and DM + Baicalin groups. Scale bars = 200 μm in A, 1 μm in B, Scale bars = 100 μm in I. \*p < 0.05, \*\*p < 0.01, \*\*\*p < 0.001 compared with control group; #p < 0.05, ##p < 0.01, ###p < 0.001 compared with DM group.

hyperglycemia in diabetic mice (Figure 2(i)), and this was also reflected in our renal tubular damage scores (Figure 2(j)). Using double immunofluorescent staining for PCNA (red) and lotus tetragonolobus lectin (LTL) (green) expressions in the proximal tubules [43], we observed diabetes increased renal tubular cell proliferation, while baicalin treatment inversely inhibited proliferation (Figure 2(i,k)).

Interestingly, baicalin treatment also inhibited diabetes-induced tubular cell apoptosis, as revealed by caspase-9 immunofluorescent staining (Figure 2(i,l)). The increase in cell proliferation and apoptosis induced by diabetes and their subsequent reduction following baicalin treatment was evident in Fas, caspase-9 and PCNA expressions, as revealed by western blot (Figure 2(m-n)). In addition, baicalin treatment also



inhibited diabetes-induced tubular cell Atg7 activation (Supplementary Figure 1). In sum, these findings indicate that baicalin could meliorate hyperglycemia-induced lesions in the renal glomeruli and tubules of diabetic mice.

### **Baicalin treatment alleviates inflammation and oxidative stress in diabetic renal tissues**

Inflammation and oxidative stress are closely associated with diabetic nephropathy [44,45]. Hence, we examined whether baicalin affected both processes in our model. CD3 and CD68 immunohistological stainings were used to show the presence of inflammatory cells, CD3<sup>+</sup> for lymphocytes, and CD68<sup>+</sup> for macrophages. We determined that baicalin treatment significantly reduced the presence of these inflammatory cells in the diabetic kidney (Figure 3(a-c)). Immunofluorescent staining for P65, a key mediator in NF- $\kappa$ B signaling, revealed that baicalin could repress P65 expression, which was enhanced in the diabetic kidney (Figure 3(a,d)). RT-qPCR analysis revealed that baicalin treatment inhibited TNF- $\alpha$  and NLRP3 expressions which was enhanced in the diabetic kidney, but did not affect the enhanced MCP-1 expression (Figure 3(e)). Western blot analysis revealed that baicalin reduced CD3, CD68, and P65 expressions that were enhanced by diabetes and inversely increased I $\kappa$ B- $\alpha$  expression (figure 3(f-g)). The results suggest that baicalin treatment inhibited diabetes-induced kidney inflammation though regulating NF- $\kappa$ B signaling.

Analysis of MDA, SOD, and CAT activities revealed baicalin inhibited MDA activity that was increased by diabetes, while increased SOD and CAT activities that are repressed (Figure 4(a-c)). Western blot showed that Nrf2 (a key anti-oxidative protein) was inhibited by baicalin in diabetic mice (Figure 4(d-e)). RT-qPCR analysis also revealed that CuZn-SOD, Mn-SOD, CAT, and GPX expressions were down-regulated in diabetic mice but restored following baicalin treatment (figure 4(f)). These results suggest that baicalin could affect oxidative stress in kidney of diabetic mice.

### **Baicalin could inhibit renal fibrosis induced by diabetes mellitus**

Transverse sections of control and diabetic kidneys were stained with Masson and Sirius red dyes to demonstrate the extent of fibrosis in these kidneys. The staining show there was more collagens in diabetic than control kidneys, but the presence of these collagens was significantly reduced following baicalin treatment (Figure 5(a-c)). Renal tubular epithelial cells are the major components of the renal parenchyma and usually the target of kidney injury. Some renal tubular epithelial cells undergo EMT process and transformed into activated myofibroblasts, which is one of the important mechanisms of renal fibrosis progression [46,47]. Immunofluorescent staining revealed that the high expression of  $\alpha$ -SMA (indicating activated myofibroblasts) in diabetic renal tissues was inhibited by baicalin treatment (Figure 5(a, d)). Next, we determined the expression levels of profibrotic proteins related EMT in diabetic kidneys, with and without baicalin treatments (figure 5(f-k)). Western blot analysis revealed that E-Cadherin was down-regulated, while  $\alpha$ -SMA and  $\beta$ -catenin were up-regulated in diabetic kidneys, but expression of these proteins were restored following baicalin treatment (figure 5(f-g)). We also found that baicalin treatment could significantly reverse the mRNA levels of  $\alpha$ -SMA, fibronectin (FN), fibroblast-specific protein-1 (FSP-1) (Figure 5(j)). Previous studies manifested that the major pathway leading to renal fibrosis is TGF- $\beta$ 1/Smad signaling pathway [48,49]. A critical effect of TGF- $\beta$ 1 is to induce epithelial-mesenchymal transition (EMT), directly promote the production of ECM and transdifferentiate tubular epithelial cells to fibroblast [50]. Immunofluorescent staining indicated that that baicalin regressd the enhanced expression of TGF- $\beta$ 1 in diabetic renal tissues (Figure 5(a,e)). In addition, TGF- $\beta$ 1 and p-smad2/3 were highly expressed, while MMP13 weakly expressed in diabetic kidneys. Again, baicalin treatment could significantly reverse these alterations (Figure 5(h-i)). We also found that baicalin treatment could significantly reverse the

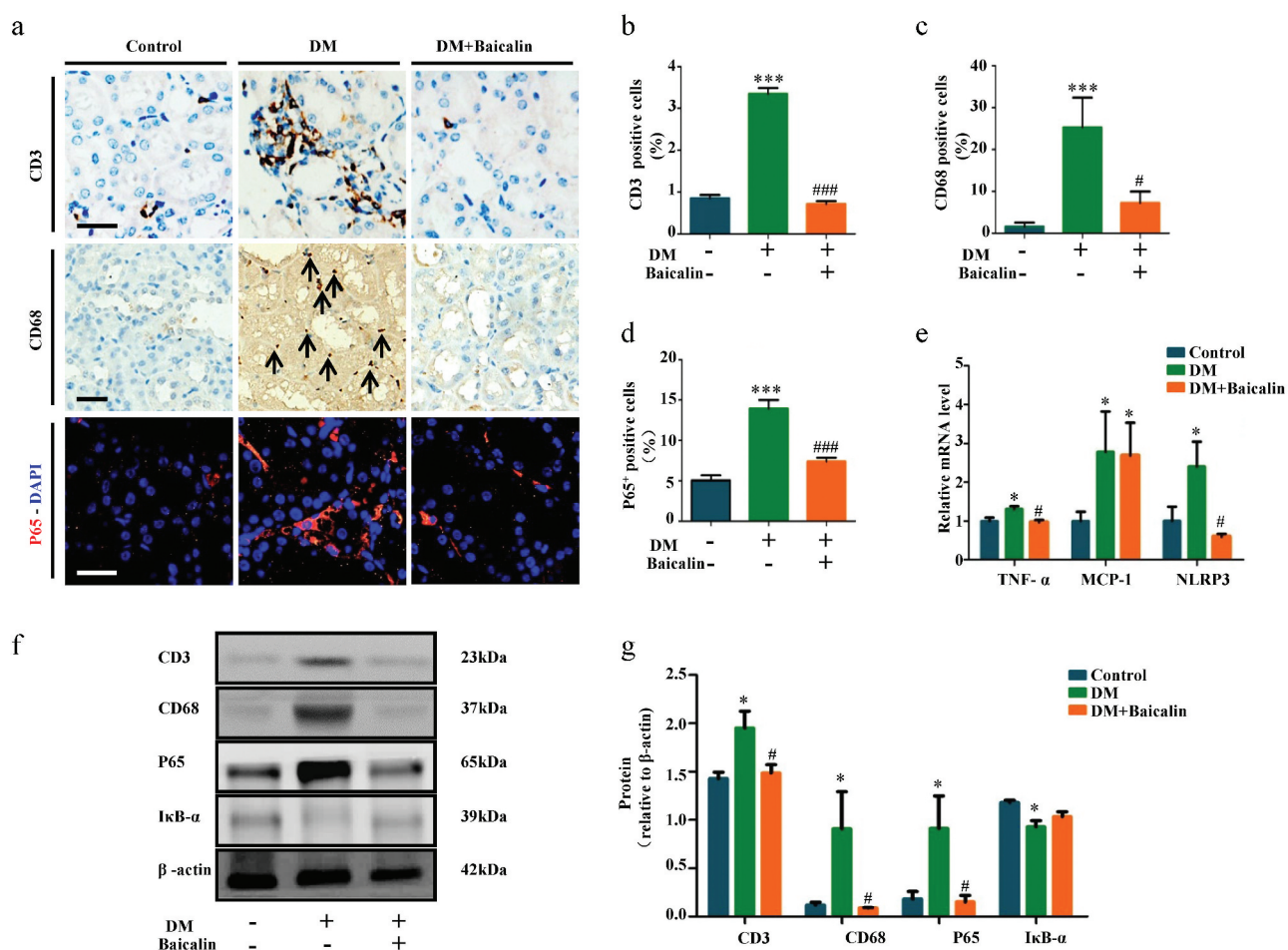


**Figure 3.** Assessments of inflammation in renal tissues of diabetic mice with baicalin treatment.

**a:** Representative Immunohistological staining for CD3, CD68 and P65 in kidney tissues of control, DM and DM + Baicalin treated mice. **b-d:** Bar charts showing the percentage of CD3<sup>+</sup> (B), CD68<sup>+</sup> (C) and P65<sup>+</sup> (D) cells in kidney tissue sections of control, DM and DM + Baicalin treated mice. **e:** RT-qPCR showing extent of TNF- $\alpha$ , MCP-1 and NLRP3 expressions in control, DM and DM + Baicalin kidneys. **f-g:** Western blot showing extent of CD3, CD68, P65 and I $\kappa$ B- $\alpha$  expressions. Scale bars = 100  $\mu$ m in A. \* $p$  < 0.05, \*\* $p$  < 0.01, \*\*\* $p$  < 0.001 compared with control group; # $p$  < 0.05, ## $p$  < 0.01, ### $p$  < 0.001 compared with DM group.

expression of Smad2, Smad3 and Smad7 induced by diabetes at mRNA levels (Figure 5(k)). These findings suggested that baicalin indeed could alleviate renal fibrosis by inhibiting TGF- $\beta$ 1-induced EMT in diabetes.

### Baicalin treatment alleviates kidney injury through the inhibition of Klotho hypermethylation

Epigenetic modifications, such as DNA methylation, is intimately associated with development of renal interstitial fibrosis [51]. Using western blot approach, we demonstrated that diabetes and baicalin did not affect DNA

methyltransferases 1 (DNMT-1) expression. However, diabetes increased Dnmt3a and Dnmt3b expressions and baicalin treatment was able to inhibit the Dnmt3a increase (Figure 6(a-b)). RT-qPCR revealed that baicalin treatment was able to reduce Dnmt3a and Dnmt3b expressions, that were enhanced by diabetes, at the mRNA level (Figure 6(c)). Interestingly, there were no significant change in the methylation of TGF- $\beta$ 1, no matter in presence of hyperglycemia or baicalin (Figure 6(d)).

Klotho, which could inhibit TGF- $\beta$ 1 signaling and suppresses renal fibrosis, is an essential homeostatic modulator of renal physiological function. Harmful external factors could activate

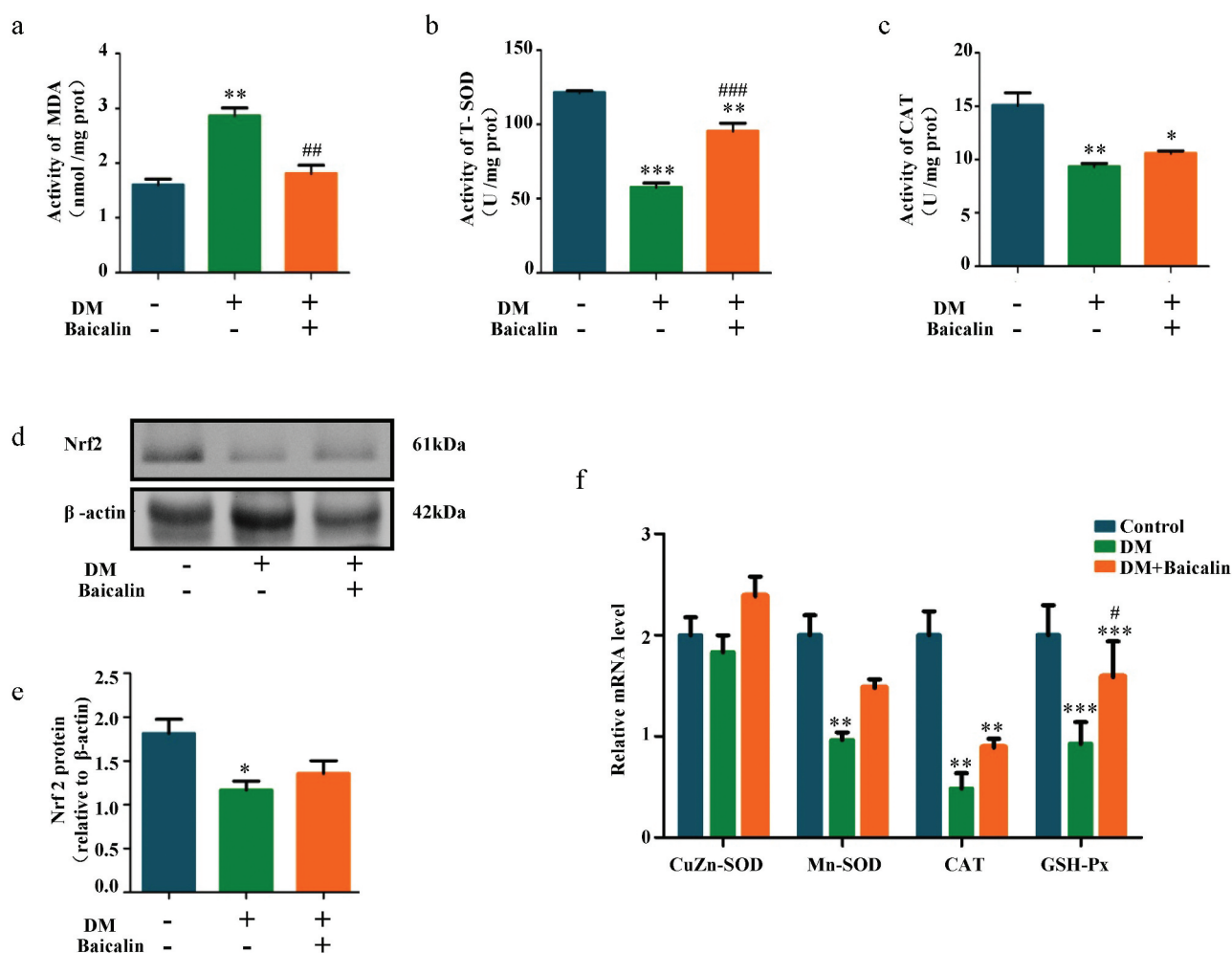


**Figure 4.** Assessments of oxidative stress in renal tissues of diabetic mice with baicalin treatment.

**a-c:** Bar charts showing MDA (A), SOD (B) and CAT (C) activities in control, DM and DM + Baicalin kidney tissues. **d-e:** Western blot showing extent of Nrf2 expressions in control, DM and DM + Baicalin treated kidney tissues. **f:** RT-qPCR showing the extent of CuZn-SOD, Mn-SOD, CAT and GPX expressions. \* $p < 0.05$ , \*\* $p < 0.01$ , \*\*\* $p < 0.001$  compared with control group; # $p < 0.05$ , ## $p < 0.01$ , ### $p < 0.001$  compared with DM group.

DNMT-1 expression, that in turn hypermethylate and silence Klotho expression [52,53]. Our western blot analysis revealed that baicalin treatment could restore Klotho expression that was repressed in the diabetic kidney (Figure 6(e-f)). This was also verified by RT-qPCR (Figure 6(g)). Furthermore, diabetes increased Klotho methylation but this increase was suppressed after baicalin treatment (Figure 6(h)). We also discovered that the methylation level at all CpG sites (CpG1 – 8) in the Klotho promoter was elevated in diabetic mice, and baicalin treatment was only able to repress methylation at the CpG1, CpG3, CpG4 and CpG5 sites (Figure 6(i)).

We investigated the importance of Klotho by silencing its expression in high glucose (HG)

microenvironment using Klotho-specific siRNA in human HK2 renal tubular cells (Figure 7). We found HG inhibited Klotho, but promoted Dnmt3a and Dnmt3b expressions *in vitro*. The baicalin administration could reverse these changes as same as *in vivo* (Figure 7(a-b)). The Klotho-specific siRNA could inhibit Klotho after HG and baicalin administration (Figure 7(c-d)). Similarly, our immunofluorescent staining revealed that silencing Klotho expression re-elevated TGF- $\beta$ 1,  $\alpha$ -SMA,  $\beta$ -catenin, and P65 expressions as compared with HK2 cells maintained under high glucose plus baicalin (Figure 7(e-j)), and (Supplementary Figure 2). It also inhibited E-cadherin expressions after baicalin treatment restored E-cadherin expression that

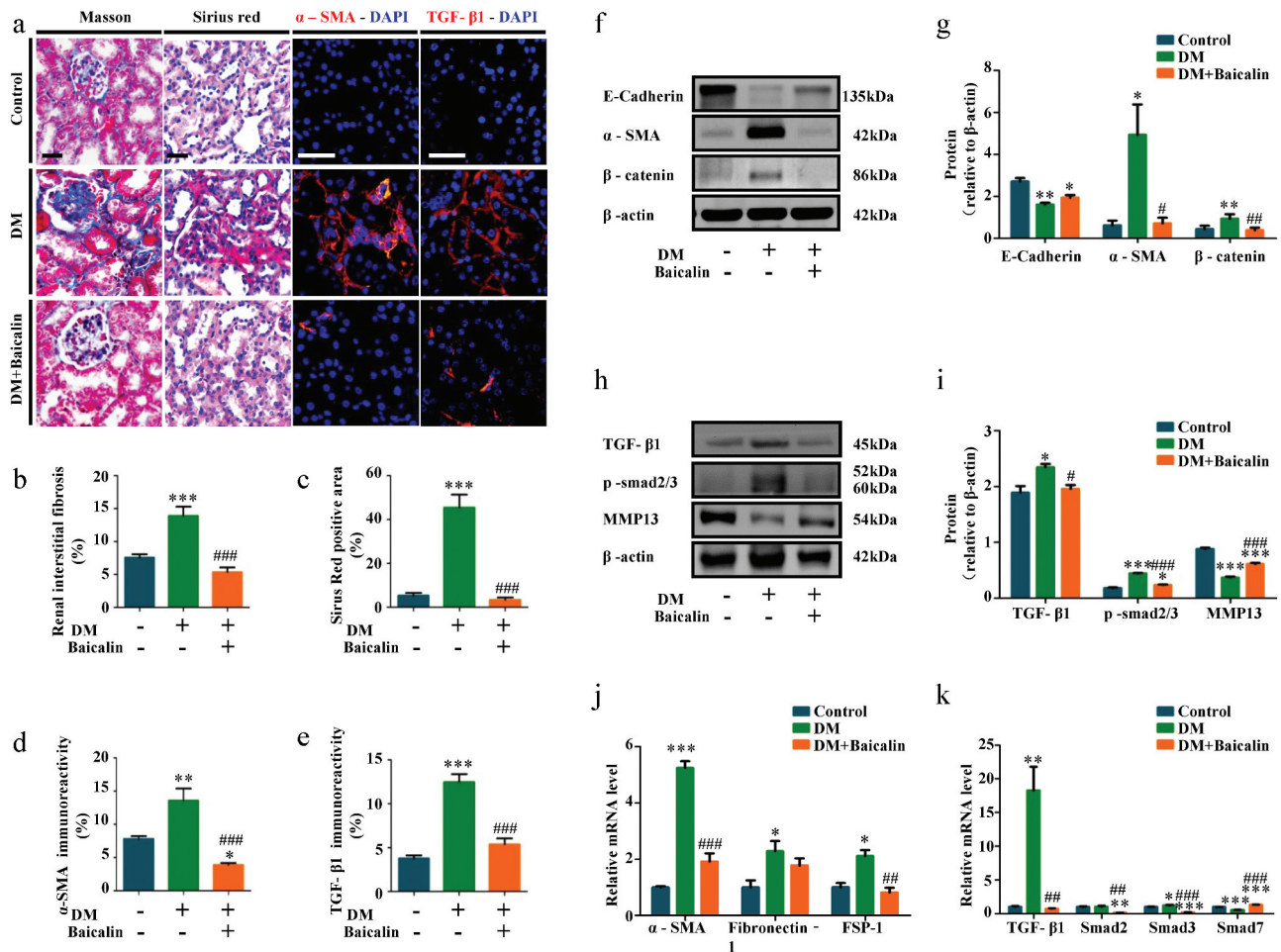


**Figure 5.** Assessments of renal interstitial fibrosis and profibrotic-associated proteins in diabetic mice with baicalin treatment.

**a:** Representative micrographs of kidney tissues stained using Masson's, Sirius red stains and also immunofluorescent staining for  $\alpha$ -SMA and TGF- $\beta$ 1 from control, DM and DM + Baicalin mice. **b-e:** Bar charts showing Masson's (B), Sirius red (C),  $\alpha$ -SMA (D) and TGF- $\beta$ 1 (E) staining intensities. **f-i:** Western blot showing the extent of E-Cadherin,  $\alpha$ -SMA,  $\beta$ -catenin, TGF- $\beta$ 1, p-smad2/3, and MMP13 expressions in control, DM and DM + Baicalin treated kidney tissues. **j-k:** RT-qPCR showing the extent of  $\alpha$ -SMA, FN, FSP-1, TGF- $\beta$ 1, Smad2, Smad3 and Smad7. Scale bars = 100  $\mu$ m in A. \* $p$  < 0.05, \*\* $p$  < 0.01, \*\*\* $p$  < 0.001 compared with control group; # $p$  < 0.05, ## $p$  < 0.01, ### $p$  < 0.001 compared with DM group.

was repressed under high glucose (Figure 7(i)). These findings confirm that hypermethylation of the Klotho promoter plays an important role in baicalin's ability to inhibit renal fibrosis.

## Discussion

Diabetes mellitus is a disorder that developed when our body can not make sufficient insulin or utilize insulin appropriately. As diabetes induced by STZ injection is often referred to as type 1 diabetes in rodents because STZ targets

pancreatic beta cells [54,55]. In this study, the ability of baicalin to treat diabetic kidney disease was extensively examined in STZ induced type 1 diabetes mice model. We used baicalin at 40 mg/kg/day to observe the biochemical and molecular changes induced by high blood glucose levels in diabetic mice. We determined that baicalin could normalize the changes induced by hyperglycemia. Specifically, the abnormally elevated biochemical index (water consumption, urine volume, BUN, serum creatine, and UACR) for renal function in diabetic mice was reverted back to normal

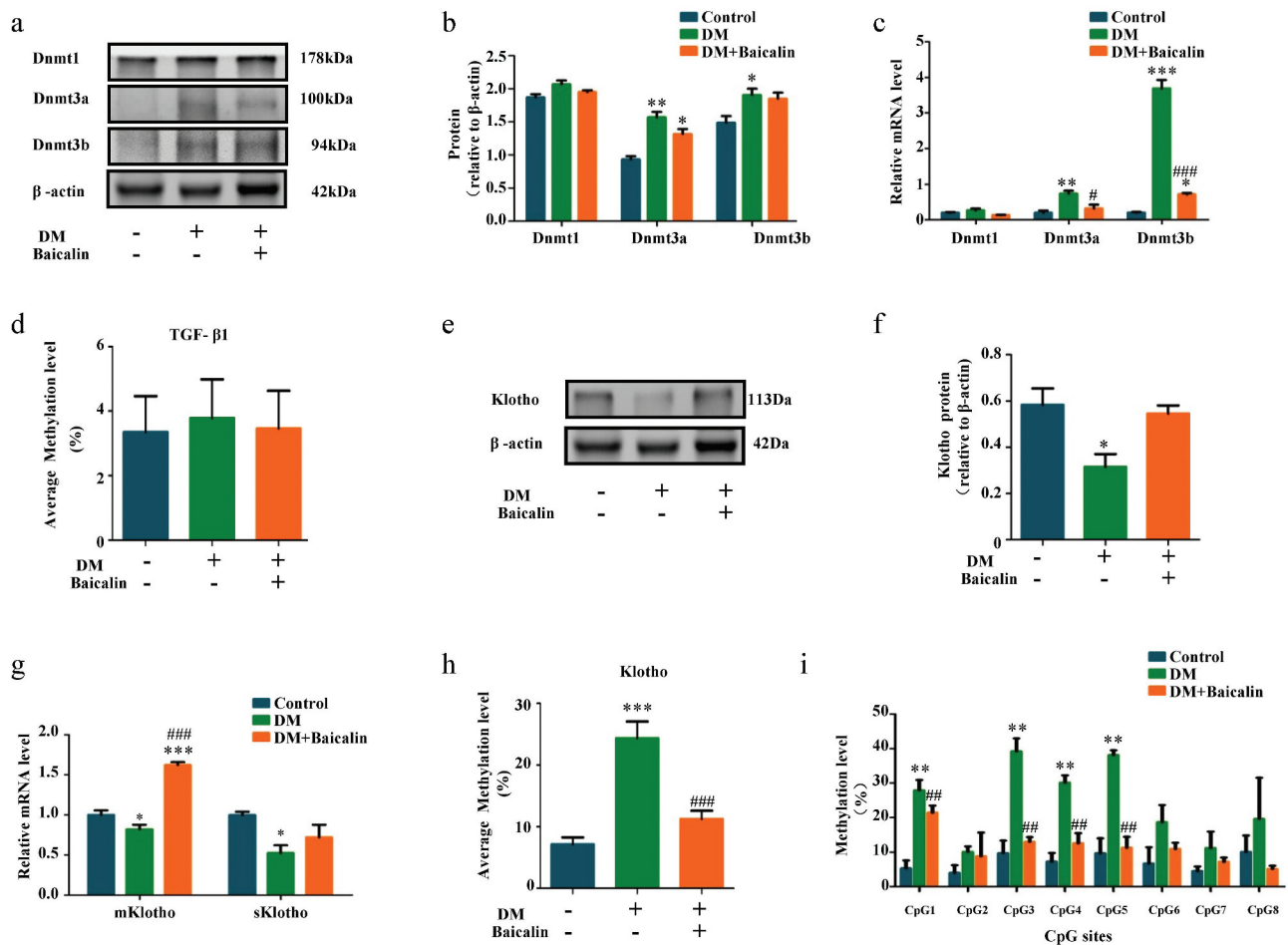


**Figure 6.** DNMT expressions and Klotho promoter hypermethylation in diabetic kidneys with baicalin treatment.

**a-b:** Western blot and **c:** RT-qPCR showing extent of Dnmt1, Dnmt3a, and Dnmt3b expression in control, DM and DM + Baicalin treated kidneys. **d:** Bar chart demonstrating the average methylation levels of TGF-β1 in control, DM and DM + Baicalin kidney tissues. **e-f:** Western blot showing the extent of Klotho expression in control, DM and DM + Baicalin treated kidney tissues. **g:** RT-qPCR showing mKlotho and sKlotho expressions in control, DM and DM + Baicalin treated kidney tissues. **h:** Bar chart demonstrating the average methylation levels of Klotho in control, DM and DM + Baicalin kidney tissues. **i:** Bar chart showing the methylation levels of CpG1, CpG2, CpG3, CpG4, CpG5, CpG6, CpG7, and CpG8. \* $p < 0.05$ , \*\* $p < 0.01$ , \*\*\* $p < 0.001$  compared with control group; # $p < 0.05$ , ## $p < 0.01$ , ### $p < 0.001$  compared with DM group.

following baicalin treatment (Figure 1). We then assessed how these improved physiological tests correlated with the histology of the renal glomeruli and tubules in diabetic mice.

Histological examinations and RT-qPCR revealed that baicalin treatment ablated and partially reversed the increase in mesangial matrix indexes and mean GBM thickness induced by diabetes (Figure 2(a-f)). This indicates that baicalin treatment could partially reverse mesangial expansion and basement membrane thickening in diabetic mice. Nephrin is a transmembrane protein that is localized in slit diaphragms as a critical component of the renal

glomerular filtration barrier [56]. While WT1 is a zinc-finger-containing transcription factor that could directly activate nephrin, acting like a key regulator in podocyte function [56,57]. We determined that baicalin treatment could reverse the inhibitory effects of diabetes on nephrin and WT1 expressions (Figure 2(g-h)). This suggests that the positive effects of baicalin on nephrin and WT1 expressions may have partially normalized the reduced glomerular filtration rate induced by diabetes. There was improvement in renal tubules ions, organic molecules, water, and vitamins reabsorptions after the treatment of baicalin compared with

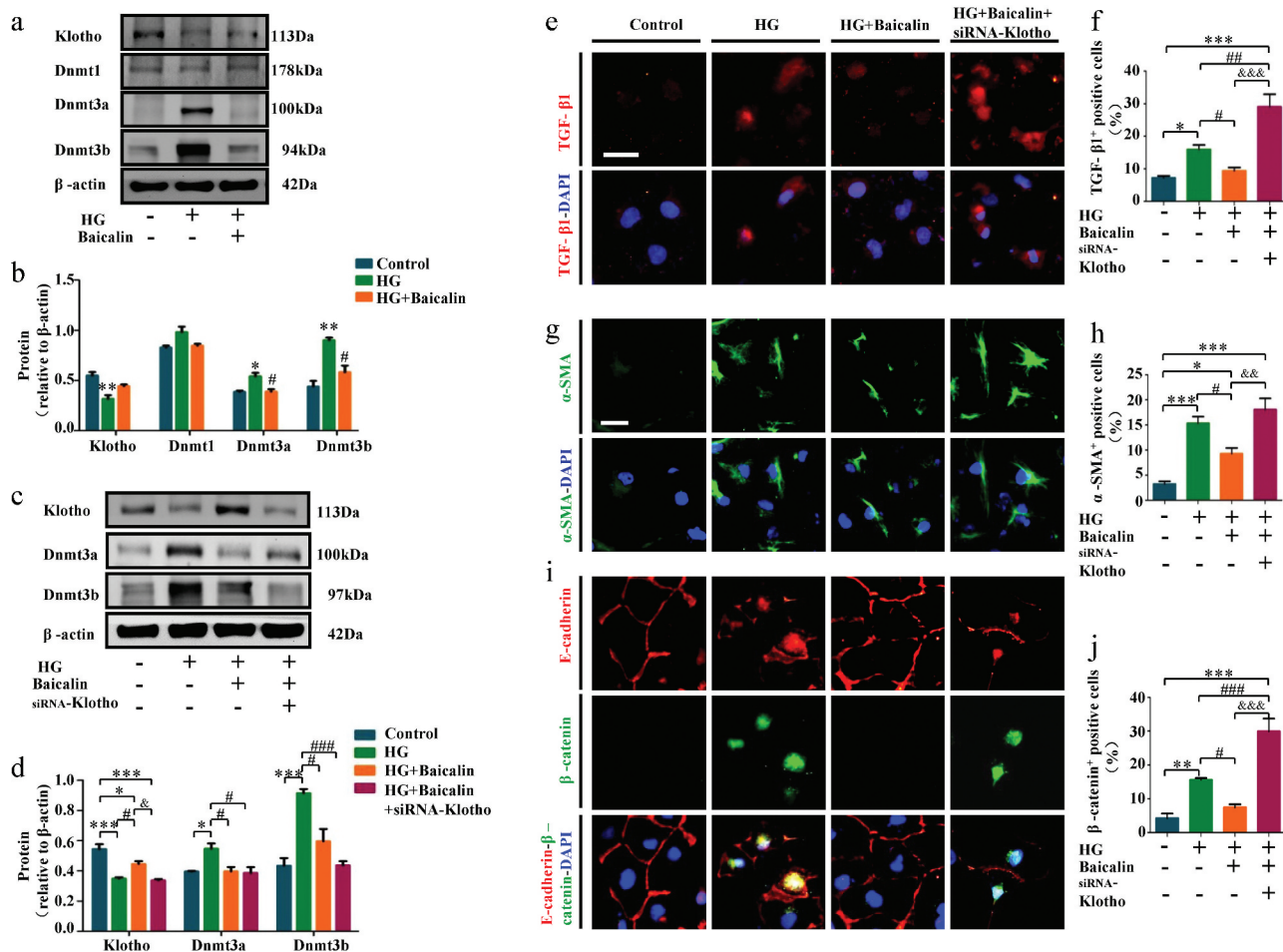


**Figure 7.** Klotho, DNMT and profibrotic-associated proteins expressions after silencing Klotho in HK2 cells treated with high glucose and baicalin.

**a-b:** Western blots showing extent of Klotho, Dnmt1, Dnmt3a, and Dnmt3b expressions in HK2 cells. **c-d:** Effects of silencing Klotho on Dnmt3a and Dnmt3b expressions. **e:** Representative micrographs of HK2 cells immunofluorescently stained for TGF-β1. **f:** Bar chart showing the percentage comparisons of TGF-β1<sup>+</sup> HK2 cells. **g:** Representative micrographs of HK2 cells immunofluorescently stained for α-SMA. **h:** Bar chart showing the percentage comparisons of α-SMA<sup>+</sup> HK2 cells. **i:** Representative micrographs of HK2 cells immunofluorescently stained for E-cadherin, β-catenin, E-cadherin and β-catenin expression in control, HG, HG + Baicalin, and HG + Baicalin + siRNA-Klotho groups. **j:** Bar charts showing percentage of β-catenin<sup>+</sup> HK2 cells. Scale bars = 20 μm in E, G and I. \*p < 0.05, \*\*p < 0.01, \*\*\*p < 0.001 compared with control group; #p < 0.05, ##p < 0.01, ###p < 0.001 compared with HG group; &p < 0.05, &&p < 0.01, &&&p < 0.001 compared with HG + Baicalin group.

the diabetes mice. The renal tubular damage score and apoptosis increased in the diabetic kidney but this was significantly reversed following baicalin exposure, indicating that baicalin could protect the renal tubules from the deleterious effects of hyperglycemia (Figure 2(i-n)).

Inflammation undoubtedly plays a crucial role in the development of diabetic kidney disease [58]. Hence, we investigated the bioactivity of baicalin on the inflammatory responses induced by diabetes mellitus (Figure 3). In the diabetic kidney, there were increased presence of CD68<sup>+</sup>

macrophage and CD3<sup>+</sup> lymphocytes in the tissues but this was significantly decreased when following baicalin treatment. This implies that baicalin can exert anti-inflammatory responses in diabetic kidney. Moreover, baicalin also affected NF-κB signaling by increasing P65, TNF-α, and NLRP3 expression while decreasing IκB-α expression, which could explain how inflammation induced by diabetes was reversed by baicalin [45].

Oxidative stress is associated with activation of NF-κB and TGF-beta1/Smad3 signaling, and also inflammatory cytokines [44]. Excessive ROS are

produced when there are too many electrons, which are converted into hydrogen peroxide by mitochondrial matrix enzymes; manganese superoxide dismutase (MnSOD or SOD2) and copper/zinc superoxide dismutase (Cu/ZnSOD or SOD1). We observed that baicalin treatment could restore the reduced SOD, CAT, and GPX bioactivities, increased MDA activity, and decreased Nrf2 (essential anti-oxidative gene) expression. This implies that baicalin can exert anti-oxidative responses in diabetic kidney.

Many evidence demonstrated that renal interstitial fibrosis was the most important pathological feature of DN [59]. In our experiments, we investigated the effect of baicalin on renal interstitial fibrosis caused by diabetes. These results showed that baicalin could obviously reverse renal interstitial fibrosis with diabetes. In kidney fibrosis, some tubular epithelial cells undergo EMT, in which the epithelial cells transform into mesenchyme [60]. When kidney fibrosis occurs, tubular epithelial cells gave rise to more than one-third of disease-associated fibroblasts [61]. This suggests that undergoing EMT in renal tubular epithelial cells plays an important role in the process of kidney injury and fibrosis. Our study indicates that baicalin could inhibit renal fibrosis by suppressing the EMT in renal tubular epithelial cells, which was further verified on EMT-associated proteins using western blot (Figure 5f-g)). Oxidative stress and inflammation enhanced by high glucose environment can induce the expression of TGF- $\beta$ 1 [62–64], which was identified as involved in the pathogenesis of diabetic nephropathy. TGF- $\beta$ 1 is generally accepted as the main activator of renal fibrosis, by inducing epithelial-mesenchymal transition (EMT) where renal cells are continuously replaced by fibroblasts [46,65]. Consequently, we investigated the link between TGF- $\beta$ 1-induced EMT and fibrosis progression in the diabetic kidney. We observed that baicalin could inhibit renal fibrosis by suppressing TGF- $\beta$ 1-induced EMT (Figure 5(f-i)). Diabetes altered the expression of EMT-associated and TGF- $\beta$ 1/smads mRNA which include: E-cadherin,  $\alpha$ -SMA,  $\beta$ -catenin, MMP13, FN, TGF- $\beta$ 1, p-smad2/3, Smad2, Smad3, and Smad7. Baicalin treatment could restore

and normalize the expression of these proteins which are mediators of kidney fibrosis [66]. This suggests that baicalin can protect the diabetic kidney from fibrosis by inhibiting TGF- $\beta$ 1-induced EMT in diabetes. DNA methylation has been closely associated with renal fibrosis [51]. We initially hypothesized that baicalin's protective effect might be attributed to its effect on DNA methylation of TGF- $\beta$ 1. However, this does not appear to be the case as there was no significant in changes in TGF- $\beta$ 1 methylation with baicalin treatment.

As a single transmembrane protein expressed mainly in the kidney, Klotho is an anti-aging protein identified in 1997 [67]. Recently, studies have shown that the Klotho can improve renal interstitial fibrosis by inhibiting TGF $\beta$ 1 signaling [9,68]. In addition, it has been reported that Dnmt1/3a aberrations would cause fibrosis and the loss of Klotho expression [52]. We then examined expression of Klotho because renal injury decreases the expression of this anti-aging protein, which is simultaneously coupled with aberrant DNA methylation. Presently, we confirmed that Klotho methylation was up-regulated in diabetes while Klotho expression was correspondingly down-regulated (Figure 6(h-i)). However, this was dramatically reversed following baicalin treatment, which principally occurred in the CpG3-5 methyl groups at the CpG dinucleotides. To further verify this observation, we silenced Klotho expression using Klotho specific-siRNAs in human HK2 renal tubular cells (Figure 7). The results revealed that silencing Klotho resulted in a reduction of baicalin's anti-fibrosis effects in the diabetic kidney.

In our previous study [28], we demonstrated that the Baicalin administration attenuated hyperglycemia-induced malformation of offspring, and the kidney injury occurred in maternal mice injected with streptozotocin. Therefore, we did not change the gender of mice in this study. There was not mouse gender difference in this study that we explored the underlying mechanism. So, we do not want to give rise to any gender biases.

In Figure 8, we have proposed the molecular mechanisms of baicalin's bioactivity in a diabetic mouse model and human kidney cell line.

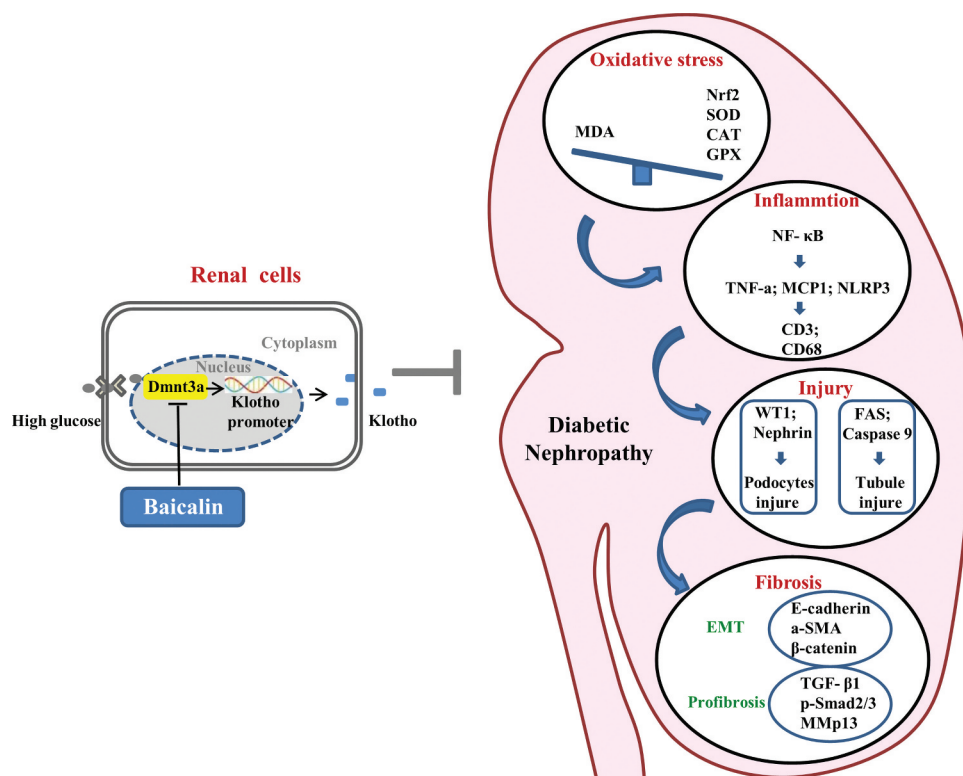


**Figure 8.** Model depicting how baicalin treatment suppresses hyperglycemia-induced renal interstitial fibrosis in diabetic mice.

Firstly, we demonstrated that the diabetic renal function indexes and pathologic changes (such as injury in the glomeruli and tubules) were significantly alleviated by baicalin treatment. Next, we manifested that baicalin protected the kidney from suppressing excessive ROS production and inflammation induced by diabetes mellitus. DNA methylation is crucial on regulating the expression of Klotho that normally counterbalances the action of TGF- $\beta$  signaling, which could induce renal tubular epithelial cells to undergo EMT and potentially activate renal fibrosis in the diabetic kidney. In this regulatory process, a key factor is the activation of the Klotho promoter controlled by Dmmt3a. In conclusion, our study, for the first time, revealed the methylation target site of baicalin on diabetic kidney disease and baicalin could be a potential candidate compound for preventing the type 1 diabetes induced kidney injury.

## Acknowledgments

This study was supported by NSFC grant (31771331, 81741016), Science and Technology Planning Project of Guangdong Province (2017A050506029, 2017A020214015, 2016B030229002), Science and Technology Program of Guangzhou (201710010054), Guangdong Natural Science Foundation (2016A030311044), Science and Technology Planning Project of Guangdong Province (A2020503), Project of National University Students “Challenge Cup” (18112003).

## Funding

This work was supported by the National Natural Science Foundation of China [31771331, 81741016]; Science and Technology Program of Guangzhou [201710010054]; Project of National University Students “Challenge Cup” [18112003]; Guangdong Natural Science Foundation [2016A030311044]; Science and Technology Planning Project of Guangdong Province [A2020503]; Science and Technology Planning Project of Guangdong Province [2017A050506029, 2017A020214015, 2016B030229002].



## Data availability statements

The data sets used and analyzed during the current study are available from the corresponding author on reasonable request.

## Author contributions

X.Z., G.W., L.Y., Y.P., R.L. and J.L. performed the experiments and collected the data; X.Z., G.W., L.W. and X. Y. designed the study and analyzed the data; K.L. and X. Y. wrote manuscript.

## Disclosure statement

The authors declare that there are no competing financial interests.

## Funding

This work was supported by the National Natural Science Foundation of China [31771331, 81741016]; Science and Technology Program of Guangzhou [201710010054]; Project of National University Students “Challenge Cup” [18112003]; Guangdong Natural Science Foundation [2016A030311044]; Science and Technology Planning Project of Guangdong Province [A2020503]; Science and Technology Planning Project of Guangdong Province [2017A050506029, 2017A020214015, 2016B030229002].

## References

- [1] Nasri H, Rafieian-Kopaei M. Diabetes mellitus and renal failure: prevention and management. *J Res Med Sci.* 2015;20:1112–1120.
- [2] Hadjadj S, Cariou B, Fumeron F, et al. Death, end-stage renal disease and renal function decline in patients with diabetic nephropathy in French cohorts of type 1 and type 2 diabetes. *Diabetologia.* 2016;59:208–216.
- [3] Forbes JM, Cooper ME. Mechanisms of diabetic complications. *Physiol Rev.* 2013;93:137–188.
- [4] Wang W, Sun W, Cheng Y, et al. Role of sirtuin-1 in diabetic nephropathy. *J Mol Med (Berl).* 2019;97:291–309.
- [5] Magee C, Grieve DJ, Watson CJ, et al. Diabetic Nephropathy: a Tangled Web to Unweave. *Cardiovasc Drugs Ther.* 2017;31:579–592.
- [6] Yesil-Devecioglu T, Dayan A, Demirtunc R, et al. Role of DNA repair genes XRCC3 and XRCC1 in predisposition to type 2 diabetes mellitus and diabetic nephropathy. *Endocrinol Diabetes Nutr.* 2019;66:90–98.
- [7] Badal SS, Danesh FR. New insights into molecular mechanisms of diabetic kidney disease. *Am J Kidney Dis.* 2014;63:S63–83.
- [8] Zou D, Wu W, He Y, et al. The role of klotho in chronic kidney disease. *BMC Nephrol.* 2018;19:285.
- [9] Doi S, Zou Y, Togao O, et al. Klotho inhibits transforming growth factor-beta1 (TGF-beta1) signaling and suppresses renal fibrosis and cancer metastasis in mice. *J Biol Chem.* 2011;286:8655–8665.
- [10] Palm F, Cederberg J, Hansell P, et al. Reactive oxygen species cause diabetes-induced decrease in renal oxygen tension. *Diabetologia.* 2003;46:1153–1160.
- [11] Stenvinkel P, Karimi M, Johansson S, et al. Impact of inflammation on epigenetic DNA methylation - a novel risk factor for cardiovascular disease? *J Intern Med.* 2007;261:488–499.
- [12] Dorotea D, Kwon G, Lee JH, et al. A pan-NADPH Oxidase Inhibitor Ameliorates Kidney Injury in Type 1 Diabetic Rats. *Pharmacology.* 2018;102:180–189.
- [13] Domingueti CP, Dusse LMSA, Carvalho MDGA, et al. Diabetes mellitus: the linkage between oxidative stress, inflammation, hypercoagulability and vascular complications. *J Diabetes Complications.* 2016;30(4):738–745.
- [14] Buitinga M, Callebaut A, Marques Camara Sodre F, et al. Inflammation-Induced Citrullinated Glucose-Regulated Protein 78 Elicits Immune Responses in Human Type 1 Diabetes. *Diabetes.* 2018;67:2337–2348.
- [15] Wang P, Cao Y, Yu J, et al. Baicalin alleviates ischemia-induced memory impairment by inhibiting the phosphorylation of CaMKII in hippocampus. *Brain Res.* 2016;1642:95–103.
- [16] Wang CZ, Zhang CF, Chen L, et al. Colon cancer chemopreventive effects of baicalein, an active enteric microbiome metabolite from baicalin. *Int J Oncol.* 2015;47:1749–1758.
- [17] Wang F, Xu Z, Ren L, et al. GABA A receptor subtype selectivity underlying selective anxiolytic effect of baicalin. *Neuropharmacology.* 2008;55:1231–1237.
- [18] Baek JS, Hwang CJ, Jung HW, et al. Comparative pharmacokinetics of a marker compound, baicalin in KOB extract after oral administration to normal and allergic-induced rats. *Drug Deliv.* 2014;21:453–458.
- [19] Zhang YM, Zhang YY, Bulbul A, et al. Baicalin promotes embryo adhesion and implantation by upregulating fucosyltransferase IV (FUT4) via Wnt/beta-catenin signaling pathway. *FEBS Lett.* 2015;589:1225–1233.
- [20] Yin F, Liu J, Ji X, et al. Baicalin prevents the production of hydrogen peroxide and oxidative stress induced by Abeta aggregation in SH-SY5Y cells. *Neurosci Lett.* 2011;492:76–79.
- [21] Shang H, Wei H, Yue B, et al. Microsatellite analysis in two populations of Kunming mice. *Lab Anim.* 2009;43:34–40.
- [22] Xu F, Chao T, Zhang Y, et al. Chromosome 1 Sequence Analysis of C57BL/6J-Chr1(KM) Mouse Strain. *Int J Genomics.* 2017;2017:1712530.

- [23] Zhang X, Zhu Z, Huang Z, et al. Microsatellite genotyping for four expected inbred mouse strains from KM mice. *J Gen Genom.* 2007;34:214–222.
- [24] Yu J, Liu X, Ke C, et al. Effective suckling C57BL/6, kunming, and BALB/c mouse models with remarkable neurological Manifestation for Zika Virus Infection. *Viruses.* 2017;9(7):165.
- [25] Sun SG, Li ZF, Liu J, et al. Correlation between anxiety and depression in animal models: evidence from light/dark box and tail suspension test in Kunming mice. *Chin Pharmacol Bull.* 2012;28:289–293.
- [26] Li CW, Li Q, Guo L, et al. Effect of rutin on liver function and morphology in type 1 diabetes mice induced by streptozotocin. *J Sichuan Univ Med Sci Ed.* 2018;49:384–7 and 424.
- [27] Kumar SD, Dheen ST, Tay SS. Maternal diabetes induces congenital heart defects in mice by altering the expression of genes involved in cardiovascular development. *Cardiovasc Diabetol.* 2007;6:34.
- [28] Wang G, Liang J, Gao LR, et al. Baicalin administration attenuates hyperglycemia-induced malformation of cardiovascular system.. *Cell Death Dis.* 2018;9:234.
- [29] Zhang X, Guo K, Xia F, et al. FGF23(C-tail) improves diabetic nephropathy by attenuating renal fibrosis and inflammation. *BMC Biotechnol.* 2018;18(1):33.
- [30] Lee SY, Kang JM, Kim DJ, et al. PGC1alpha activators mitigate diabetic tubulopathy by improving mitochondrial dynamics and quality control. *J Diabetes Res.* 2017;2017:6483572.
- [31] Acar N, Korgun ET, Cayli S, et al. Is there a relationship between PCNA expression and diabetic placental development during pregnancy? *Acta Histochem.* 2008;110:408–417.
- [32] Maroto M, Reshef R, Munsterberg AE, et al. Ectopic Pax-3 activates MyoD and Myf-5 expression in embryonic mesoderm and neural tissue. *Cell.* 1997;89:139–148.
- [33] Dugaiczak A, Haron JA, Stone EM, et al. Cloning and sequencing of a deoxyribonucleic acid copy of glyceraldehyde-3-phosphate dehydrogenase messenger ribonucleic acid isolated from chicken muscle. *Biochemistry.* 1983;22:1605–1613.
- [34] Wang L, Chen L, Tan Y, et al. Betaine supplement alleviates hepatic triglyceride accumulation of apolipoprotein E deficient mice via reducing methylation of peroxisomal proliferator-activated receptor alpha promoter. *Lipids Health Dis.* 2013;12:34.
- [35] Wang LJ, Zhang HW, Zhou JY, Liu Y, Yang Y, Chen XL, Zhu CH, Zheng RD, Ling WH, Zhu HL. Betaine attenuates hepatic steatosis by reducing methylation of the MTTP promoter and elevating genomic methylation in mice fed a high-fat diet. *J Nutr Biochem.* 2014;25:329–336.
- [36] Chihara Y, Rakugi H, Ishikawa K, et al. Klotho protein promotes adipocyte differentiation. *Endocrinology.* 2006;147:3835–3842.
- [37] He YQ, Li Y, Wang XY, et al. Dimethyl phenyl piperazine iodide (DMPP) induces glioma regression by inhibiting angiogenesis. *Exp Cell Res.* 2014;320:354–364.
- [38] He MY, Wang G, Han SS, et al. Nrf2 signalling and autophagy are involved in diabetes mellitus-induced defects in the development of mouse placenta. *Open Biol.* 2016;6(7):160064.
- [39] He MY, Wang G, Han SS, et al. Negative impact of hyperglycaemia on mouse alveolar development. *Cell Cycle.* 2018;17:80–91.
- [40] Jin Y, Wang G, Han SS, et al. Effects of oxidative stress on hyperglycaemia-induced brain malformations in a diabetes mouse model. *Exp Cell Res.* 2016;347:201–211.
- [41] Johanna G, Jauregui AN, Sandra MG, et al. Podocyte-specific GLUT4-deficient mice have fewer and larger podocytes and are protected from diabetic nephropathy. *Diabetes.* 2014;63:701.
- [42] Guo JK, Menke AL, Gubler MC, et al. WT1 is a key regulator of podocyte function: reduced expression levels cause crescentic glomerulonephritis and mesangial sclerosis. *Hum Mol Genet.* 2002;11:651–659.
- [43] Yamaguchi S, Morizane R, Homma K, et al. Generation of kidney tubular organoids from human pluripotent stem cells. *Sci Rep.* 2016;6:38353.
- [44] Kim J, Imig JD, Yang J, et al. Inhibition of soluble epoxide hydrolase prevents renal interstitial fibrosis and inflammation. *Am J Physiol Renal Physiol.* 2014;307:F971–80.
- [45] Wang W, Wang X, Zhang XS, et al. Cryptotanshinone attenuates oxidative stress and inflammation through the regulation of Nrf-2 and NF-kappaB in mice with unilateral ureteral obstruction. *Basic Clin Pharmacol Toxicol.* 2018;123(6):714–720.
- [46] Zhou T, Luo M, Cai W, et al. Runt-related transcription factor 1 (RUNX1) promotes TGF-beta-induced renal tubular epithelial-to-mesenchymal transition (EMT) and renal fibrosis through the PI3K Subunit p110delta. *EBioMedicine.* 2018;31:217–225.
- [47] Han WQ, Xu L, Tang XF, et al. Membrane rafts-redox signalling pathway contributes to renal fibrosis via modulation of the renal tubular epithelial-mesenchymal transition. *J Physiol.* 2018;596:3603–3616.
- [48] Agnieszka L, Mateusz S, Alicja J, et al. TGF-β1/Smads and miR-21 in Renal Fibrosis and Inflammation. *Mediators Inflamm.* 2016;2016:1–12.
- [49] Yu L, Border WA, Huang Y, et al. TGF-beta isoforms in renal fibrogenesis. *Kidney Int.* 2003;64:844–856.
- [50] Zeisberg M, Hanai J, Sugimoto H, et al. BMP-7 counteracts TGF-beta1-induced epithelial-to-mesenchymal

- transition and reverses chronic renal injury. *Nat Med.* **2003**;9:964–968.
- [51] Bontha SV, Maluf DG, Archer KJ, et al. Effects of DNA methylation on progression to interstitial fibrosis and tubular atrophy in renal allograft biopsies: a multi-omics approach. *Am J Transplant.* **2017**;17:3060–3075.
- [52] Yin S, Zhang Q, Yang J, et al. TGFbeta-incurred epigenetic aberrations of miRNA and DNA methyltransferase suppress Klotho and potentiate renal fibrosis. *Biochim Biophys Acta Mol Cell Res.* **2017**;1864:1207–1216.
- [53] Young GH, Wu VC. KLOTHO methylation is linked to uremic toxins and chronic kidney disease. *Kidney Int.* **2012**;81:611–612.
- [54] Szkudelski T. The mechanism of alloxan and streptozotocin action in B cells of the rat pancreas. *Physiol Res.* **2001**;50:537–546.
- [55] Wu J, Yan L-J. Streptozotocin-induced type 1 diabetes in rodents as a model for studying mitochondrial mechanisms of diabetic  $\beta$  cell glucotoxicity. *Diabetes Metab Syndr Obes.* **2015**;8:181.
- [56] Guo G, Morrison DJ, Licht JD, et al. WT1 activates a glomerular-specific enhancer identified from the human nephrin gene. *JASN.* **2004**;15:2851–2856.
- [57] Wagner N, Wagner KD, Xing Y, et al. The major podocyte protein nephrin is transcriptionally activated by the Wilms' tumor suppressor WT1. *JASN.* **2004**;15:3044–3051.
- [58] Eriguchi M, Bernstein EA, Veiras LC, et al. The absence of the ACE N-domain decreases renal inflammation and facilitates sodium excretion during diabetic kidney disease. *JASN.* **2018**;29:2546–2561.
- [59] Karihaloo A. Anti-fibrosis therapy and diabetic nephropathy. *Curr Diab Rep.* **2012**;12:414–422.
- [60] Cruz-Solbes AS, Youker K. Epithelial to mesenchymal transition (EMT) and endothelial to mesenchymal transition (EndMT): role and implications in kidney fibrosis. *Results Probl Cell Differ.* **2017**;60:345–372.
- [61] Tan RJ, Zhou D, Liu YH. Signaling crosstalk between tubular epithelial cells and interstitial fibroblasts after kidney injury. *Kidney Dis-Basel.* **2016**;2:136–144.
- [62] Gonzalez-Ramos M, de Frutos S, Griera M, et al. Integrin-linked kinase mediates the hydrogen peroxide-dependent transforming growth factor- $\beta$ 1 up-regulation. *Free Radic Biol Med.* **2013**;61:416–427.
- [63] González-Ramos M, Mora I, de Frutos S, et al. Intracellular redox equilibrium is essential for the constitutive expression of AP-1 dependent genes in resting cells: studies on TGF- $\beta$ 1 regulation. *Int J Biochem Cell Biol.* **2012**;44:963–971.
- [64] Sun L, Xiu M, Wang S, et al. Lipopolysaccharide enhances TGF- $\beta$ 1 signalling pathway and rat pancreatic fibrosis. *J Cell Mol Med.* **2018**;22:2346–2356.
- [65] Iwano M. EMT and TGF-beta in renal fibrosis. *Front Biosci.* **2010**;2:229–238.
- [66] Sureshbabu A, Muhsin SA, Choi ME. TGF-beta signaling in the kidney: profibrotic and protective effects. *Am J Physiol Renal Physiol.* **2016**;310:F596–F606.
- [67] Kuro-o M, Matsumura Y, Aizawa H, et al. Mutation of the mouse klotho gene leads to a syndrome resembling ageing. *Nature.* **1997**;390:45–51.
- [68] Mencke R, Olauson H, Hillebrands JL. Effects of Klotho on fibrosis and cancer: A renal focus on mechanisms and therapeutic strategies. *Adv Drug Deliv Rev.* **2017**;121:85–100.